Econ. Environ. Geol.
Vol. 29, No. 4, p. 483-493, 1996.

Geochemistry of the Daebo Granitic Batholith in the Central Ogcheon Belt, Korea : A Preliminary Report

Chang-Sik Cheong* and Ho-Wan Chang**

ABSTRACT : The tectonic environment and source characteristics of the Daebo granitic batholith in the central Ogcheon Belt were investigated based upon major and trace element geochemistry. The batholith is comprised of three granite types; a biotite granite (DBBG), K-feldspar megacryst-bearing biotite granite (DBKG), and a more mafic granodiorite (DBGD). The variations of Na and K in the granites can not be explained by simple fractional crystallization from the same primary magma. The irregular behavior of these alkali elements indicates a variety of source materials or incomplete mixing of different source materials. The large ion lithophile (LIL) element enrichment and low Ta/Hf ratios of the granites are typical characteristics of normal, calc-alkaline continental arc granitoids. Based upon REE patterns of the granites, it seems to be unreasonable to regard the felsic DBBG as a late stage differentiate formed by residual melts after the fractionation of major constituent minerals of the more mafic DBGD. Inconsistent variations in $\varepsilon_{Nd}(t)$ and LIL element concentrations of the granites preclude a mixing model between primitive melt and LIL element-enriched upper crustal materials. The irregular geochemical variation of the granites is taken to be largely inherited from an already heterogeneous source region.

PREFACE

The Phanerozoic granitoids in South Korea have been divided into two groups since the recognition of the Daebo Orogeny by Kim (1971). One group is the Triassic to Jurassic Daebo granite, and the other is the Cretaceous to Tertiary Bulguksa granite. All the Daebo granites have been considered to be Jurassic in age regardless of their geologic provinces, but sporadically their emplacement age was dated at Triassic or older (Choo, Kim, 1985; Kwon, 1988; Na, 1994).

The geochemistry of the granitoids in South Korea varies with their emplacement ages (summarized by Hong, 1987). Based on Nd and Pb isotopic signature, Kwon (1991, 1992) suggested that the geochemistry of the basement was the main control on the geochemical characteristics of the Phanerozoic granites in South Korea. Actually, the geological processes which control the geochemical characteristics of granites are more complex. The source chemistry and partial melting process principally determine the geochemistry of granites; but most geochemical features have changed through complex geological processes including magmatic differentiation, volatile fluxing, magma mixing, assimilation, and simultaneous assimilation and fractional crystallization (AFC) (Taylor, 1980; DePaolo, 1981) since the time of formation. We should accept the diverse possibilities involved in granite genesis and investigate each pluton individually. A petrogenetic model for Batholith A can, at best, be only partially applicable to Batholith B (Clarke, 1992).

The tectonic environment and source characteristics of the Daebo batholith in the central Ogcheon Belt were investigated here based upon major and trace element geochemistry.

GENERAL GEOLOGY

Various types of granitic rocks are found in the central Ogcheon Belt (Fig. 1). The granitic rocks in the central Ogcheon Belt can be divided into three groups; the Daebo batholith with so called Sinian NE-SW direction, Permian to Triassic granites distributed near the Boeun area (hereafter PTGR) (Cheong, Chang, 1996), and Cretaceous Sogrisan Granite. The

---

* Korea Basic Science Institute, Eoeun Dong 52, Yusung Ku, Taejeon 305-333, Korea

** Department of Geological Science, Seoul National University, seoul 151-742, Korea

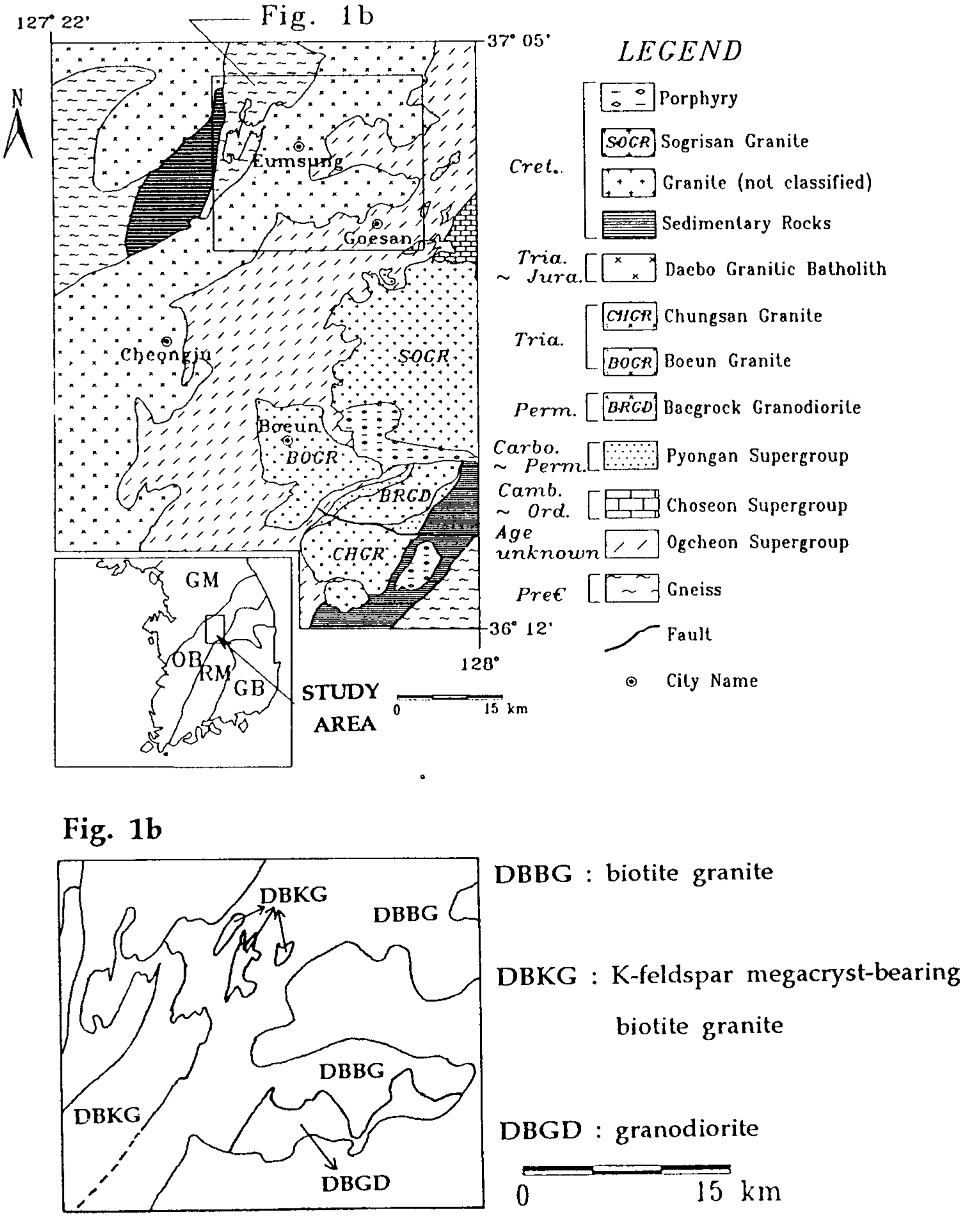

Fig. 1. Geologic map of the central Ogcheon Belt, Korea. Abbreviations: GB; Gyongsang Basin, RM; Ryongnam Massif, OB; Ogcheon Belt, and GM; Gyonggi Massif. Distribution of the Daebo granites in the Goesan-Eumsung area is shown in Fig. 1b (after Choi, in preparation).

granitic rocks were emplaced into highly deformed, undated metamorphics of the Ogcheon Supergroup. The southeastern and northwestern part of the study area is covered with Cretaceous sedimentary rocks and a Precambrian gneiss complex.

The Daebo batholith is comprised of a biotite granite, two mica granite, leucocratic granite, K-feldspar megacryst-bearing biotite granite, and a more mafic granodiorite (Fig. 1b). The first three granites show transitional variation in mineralogy and texture and can be regarded as one unit called the Daebo Biotite Granite (DBBG). K-feldspar megacryst-bearing biotite granite (DBKG) is mainly distributed in the Eumsung area, and shows a well-

Table 1. Sample datails.

Sample No.	National Grid	Description*
Daebo Biotite Granite (DBBG)		
DB1	321.4/233.3	m.g. two mica granite
DB4-1	328.2/241.1	m.g. two mica granite
DB19-1	350.4/247.5	m.g. bt granite
DB33	367.8/260.3	m.g. bt granite
DB46	382.8/262.5	m.g. bt granite
DB65	370.5/268.2	m.g. bt granite
DB89-1	336.8/236.7	m.g. bt granite
K-feldspar megacryst-bearing biotite granite (DBKG)		
DB56	376.7/259.1	Ksp megacryst-bearing bt granite
DB58	375.2/254.9	Ksp megacryst-bearing bt granite, partly foliated
DB62-1	375.1/261.4	Ksp megacryst-bearing bt granite
Daebo Granodiorite (DBGD)		
DB40	368.8/270.1	c.g. granodiorite
DB41	370.6/270.2	c.g. granodiorite
DB42	372.4/269.8	Ksp megacryst-bearing granodiorite
DB72	373.5/275.3	c.g. granodiorite
DB75	371.9/276.1	c.g. granodiorite
DB77	370.6/279.5	m.g. granodiorite

*m.g.; medium grained, c.g.; coarse grained, Ksp; K-feldspar, bt; biotite

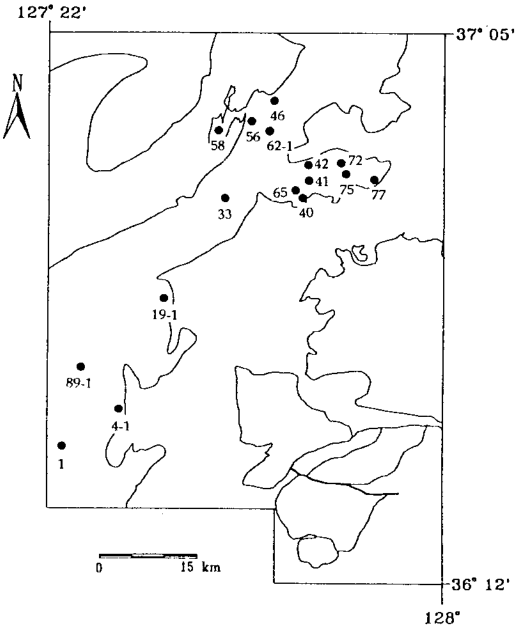

Fig. 2. Sample location map. DB letters of the sample numbers are omitted on the map.

developed foliation on its western margin. The coarse-grained granodiorite with the most mafic composition in the Daebo granites, called here as the Daebo Granodiorite (DBGD), is mainly distributed in the Goesan area.

The DBKG and the DBGD are intruded by pegmatitic portion of the DBBG. The absence of regional contact aureole between the granites, however, indicates that there is no much difference in intrusion age between them (Jin, 1995). Reported radiometric age of these granites is variable (115~193 Ma; Kim, 1971; Choo *et al*, 1979; Na, 1994), suggesting that they were formed by continuous igneous activity, although some reported ages reflect low blocking temperatures of the isotope systems and/or their resetting by Cretaceous igneous activities. Jin (1995) proposed that the main igneous activity which formed the Daebo granites in the Ogcheon Belt occurred in late Triassic or early Jurassic.

The locations and rock types of the analysed samples are given in Table 1. Sample locations are graphically presented in Figure 2.

PETROGRAPHY

Daebo Biotite Granite (DBBG)

The DBBG is typically a medium-grained, equigranular granite. Leucocratic granite mainly composed of quartz and feldspar with a small amount of biotite is only locally distributed. Modal content of muscovite is variable in the DBBG, and typical biotite granite grades into fine-grained, two mica granite with macroscopic muscovite. Typical DBBG is composed mainly of plagioclase, quartz, K-feldspar, biotite, and muscovite. Euhedral muscovite of primary magmatic origin is frequently associated with biotite. Accessory minerals are sphene, epidote, and zircon. Myrmekite is commonly found along the grain boundaries between quartz and feldspar. The myrmekite texture can be formed by local tectonic deformation (Hibbard, 1979; Simpson and Wintsch, 1989), but there are few field evidences for the tectonic movement in the DBBG. The myrmekite texture therefore could be related to the exsolution from the host K-feldspars.

K-feldspar Megacryst-bearing Biotite Granite (DBKG)

The DBKG is a K-feldspar megacryst-bearing biotite granite mainly distributed in the Eumsung area. Partly pegmatitic K-feldspar veins commonly intruded this rock. The DBKG is locally well foliated (DB 58 site), and K-feldspar megacrysts are strongly elongated in the foliated part. The strike and dip of the foliation at DB 58 site is 52 W/42 SW. But in most cases, this granite does not show a biotite foliation or consistent K-feldspar orientation. The DBKG is mainly composed of microcline, quartz, plagioclase, biotite, and hornblende. Sphene is the most abundant in accessory mineral phases. Myrmekite is rarely developed along the margins of K-feldspar grains. Two-stage crystallization is unlikely, because the megacrysts commonly contains small plagioclase inclusions which crystallized in the earlier magmatic stage (Hibbard, 1995).

Daebo Granodiorite (DBGD)

The DBGD is typically a coarse-grained granodiorite, although some fine-grained and equigranular, medium-grained textural varieties of the DBGD are locally found. This granodiorite is mainly composed of microcline, quartz, plagioclase, hornblende, and biotite with accessory minerals including sphene, zircon, epidote, and apatite. This rock often contains euhedral to subhedral K-feldspar megacrysts which are primarily microcline. Myrmekite is rarely developed along the margins of K-feldspar grains.

ANALYTICA DETAILS

Major element data were obtained by X-ray fluorescence spectrometer (XRF). Because of the presence of refractory minerals (Totland *et al.*, 1992), spectral interferences, and instrumental sensitivities, four different methods were used for trace element analysis. Samples for most trace element analyses were dissolved with a mixed acid ($HF:HClO_4:HNO_3=3:1:1$) in teflon vessels. Ba, Sc, V, and Ga concentrations were measured by inductively coupled plasma atomic emission spectrometer (ICP-AES). Ni, Nb, Y, Cs, U, Th, Pb, and rare earth elements (REE) concentrations were measured by inductively coupled plasma mass spectrometer (ICP-MS). For the measurement of Zr, Hf, and Ta concentrations, samples were fused with $LiBO_2$ and analyzed by ICP-MS. Analytical uncertainties in the data were checked by the analyses of two USGS standards (G-2 for major element analysis, W-2 for trace element analysis) and found to be 1~2% for major elements, below 10% for REEs, and around 15% for the other trace elements.

Rb, Sr, Sm, and Nd concentrations were determined by an isotope dilution technique using ^{87}Rb, ^{84}Sr, ^{149}Sm, and ^{150}Nd spike solutions. Rb, Sr, and REE fractions were separated by a cation exchange column. Sm and Nd concentrations were determined based on $^{145}Nd/^{146}Nd$ and $^{147}Sm/^{149}Sm$ ratios of REE fraction.

DATA

Major and trace element concentrations of 16 granite samples are given in Table 2.

Major element variation diagrams for the granites are shown in Figure 3. The DBGD shows wide variation in SiO_2 content, but SiO_2 contents of the other, more felsic granites vary in relatively limited ranges. TiO_2, total Fe_2O_3 (Fe_2O_3*), MgO, P_2O_5, and CaO contents are negatively correlated with SiO_2 contents in the granite samples. Al_2O_3 contents of the granites do not show a systematic pattern with SiO_2. Na_2O and K_2O contents of the granites vary widely, and do not show consistent covariation with SiO_2 contents.

Trace element variation diagrams of the granites are shown in Figure 4. In Figure 4, data of the PTGR (Cheong and Chang, 1996) are also shown for comparison. Ni, V, Sc, Sr, and Ba concentrations of the DBGD are negatively correlated with SiO_2 contents. Rb, Cs, U, and Th concentrations of the granites do not show consistent covariation with SiO_2 contents. The DBGD is more enriched in these large ion lithophile (LIL) elements than the Baegrock Granodiorite. Ta concentrations of the Daebo granites are distinctly lower than those of the PTGR, but both have similar contents of other high field strength (HFS) elements such as Nb, Hf, and Y.

On average, all the Daebo granites show rather

Table 2. Major and trace element composition of the Daebo granitic rocks from the central Ogcheon Belt, Korea. (major elements are given in wt.% oxides, trace elements in ppm).

	Daebo Biotite Granite (DBBG)							K-feldspar megacryst-bearing biotite granite (DBKG)		
	DB1	DB4-1	DB19-1	DB33	DB46	DB65	DB89-1	DB56	DB58	DB62-1
SiO_2	70.23	70.28	68.67	72.28	70.38	70.59	69.13	65.03	66.46	70.35
TiO_2	0.23	0.48	0.41	0.24	0.29	0.29	0.44	0.51	0.59	0.44
Al_2O_3	15.86	15.62	15.22	14.72	14.57	14.85	15.16	16.24	15.87	14.4
Fe_2O_3*	2.22	2.67	3.54	1.81	2.34	2.08	3.05	4.05	4.03	3.03
MnO	0.03	0.03	0.06	0.02	0.03	0.03	0.03	0.06	0.05	0.04
MgO	0.60	1.01	1.21	0.35	0.84	0.87	0.83	1.51	1.28	0.81
CaO	2.87	2.53	2.79	1.29	1.76	1.71	2.28	3.13	3.17	1.99
Na_2O	3.60	2.98	2.66	3.54	3.39	3.74	3.15	3.28	3.49	3.61
K_2O	2.53	3.63	3.88	4.39	4.32	4.11	4.01	4.25	3.20	3.36
P_2O_5	0.09	0.13	0.12	0.07	0.08	0.09	0.14	0.15	0.17	0.12
LOI	0.64	0.52	0.75	0.72	0.68	0.96	0.95	0.53	0.73	1.02
total	98.90	99.88	99.31	99.43	98.68	99.32	99.17	98.74	99.04	99.17
Ba	748	1011	1448	1035	750	1073	866	1130	1183	912
Sr	564	435	417	430	301	618	440	443	544	434
Sc	0.1	2.1	4.1	0.1	1.1	0.1	0.1	3.1	2.1	1.1
Zr	108	150	109	109	74	74	117	111	151	105
Ni	2	2	4	3	7	7	3	5	6	4
Ga	17	16	15	16	12	11	11	8	33	61
V	20	46	52	17	28	23	44	67	72	43
Hf	3.4	4.5	3.4	3.4	2.5	2.3	3.4	3.2	4.5	3.1
Nb	13	9	12	8	14	8	9	10	18	13
Ta	0.9	0.8	0.6	0.6	0.9	0.5	0.3	0.9	0.8	0.6
Rb	97	138	106	161	163	110	158	124	104	110
Y	9	9	16	6	12	7	5	15	12	8
Cs	6	6	4	5	4	3	3	2	4	3
U	1.7	1.7	1.4	1.1	3.8	1.9	1.9	1.6	2.0	2.6
Th	7	13	11	11	17	6	22	22	16	14
Pb	27	37	37	35	37	36	32	25	24	26
La	41.20	35.50	38.28	44.67	42.60	34.98	68.21	49.30	64.07	47.38
Ce	71.02	66.00	71.38	82.40	72.10	59.77	120.83	88.61	114.84	88.12
Pr	7.54	6.66	8.33	9.07	7.99	6.70	12.86	9.62	12.15	9.20
Nd	17.62	20.37	32.83	26.06	17.37	16.73	30.56	23.58	26.91	23.05
Sm	2.86	2.94	5.94	4.09	3.17	2.72	4.22	3.83	4.61	3.81
Eu	1.24	1.31	1.56	1.08	0.91	1.01	1.17	1.26	1.56	1.10
Gd	3.29	2.73	4.99	3.14	3.45	2.40	3.40	4.29	4.92	3.57
Tb	0.35	0.31	0.61	0.34	0.42	0.28	0.30	0.54	0.52	0.38
Dy	1.76	1.70	3.53	1.47	2.48	1.48	1.29	3.01	2.57	1.85
Ho	0.27	0.27	0.37	0.20	0.38	0.23	0.16	0.50	0.37	0.25
Er	0.77	0.78	1.55	0.51	1.07	0.67	0.42	1.43	1.01	0.68
Tm	0.10	0.09	0.16	0.06	0.14	0.08	0.04	0.18	0.11	0.08
Yb	0.57	0.57	1.00	0.35	0.90	0.53	0.28	1.16	0.74	0.48
Lu	0.08	0.07	0.13	0.05	0.13	0.07	0.04	0.16	0.09	0.06
ΣREE	148.7	139.3	170.7	173.5	153.1	127.7	243.8	187.5	234.5	180.0
Eu/Eu*	1.24	1.42	0.88	0.93	0.84	1.21	0.94	0.95	1.00	0.92
$(La/Yb)_N$	48.8	42.1	25.8	85.6	31.9	44.1	166.0	28.7	58.0	66.5

Table 2. Continued.

	Daebo Granodiorite (DBGD)					
	DB40	DB41	DB42	DB72	DB75	DB77
SiO_2	57.51	62.55	62.96	61.97	59.22	60.85
TiO_2	0.85	0.62	0.54	0.68	0.84	0.64
Al_2O_3	14.13	14.97	15.04	14.61	15.08	13.57
Fe_2O_3*	6.81	4.72	4.29	5.21	6.23	5.75
MnO	0.09	0.06	0.05	0.07	0.07	0.08
MgO	6.21	3.34	3.01	3.78	4.76	5.91
CaO	5.19	3.23	2.41	3.56	4.31	4.22
Na_2O	2.48	2.92	2.87	2.78	2.89	2.55
K_2O	3.77	4.79	5.38	4.16	4.11	4.09
P_2O_5	0.37	0.25	0.24	0.28	0.31	0.26
LOI	1.26	1.69	1.86	1.34	1.10	0.89
total	98.67	99.14	98.65	98.44	98.92	98.81
Ba	1558	1274	1383	1475	1479	1189
Sr	1109	805	842	952	899	774
Sc	16.1	8.1	8.1	11.1	15.1	12.1
Zr	80	154	128	209	226	104
Ni	94	49	40	51	72	115
Ga	14	9	7	27	29	9
V	147	84	73	104	135	107
Hf	2.5	4.5	3.8	5.8	6.4	3.1
Nb	7	12	10	10	11	2
Ta	0.7	1.2	1.0	0.9	1.5	0.9
Rb	126	181	189	162	181	164
Y	23	22	18	25	24	20
Cs	4	6	5	4	6	8
U	2.4	5.4	5.6	3.6	8.7	2.6
Th	17	21	15	17	10	13
Pb	29	30	30	26	27	31
La	91.64	85.09	90.49	95.72	80.68	59.19
Ce	167.26	153.94	154.57	171.01	150.15	109.63
Pr	17.57	16.01	15.60	17.40	16.03	12.27
Nd	45.84	46.83	36.63	57.89	47.73	39.06
Sm	7.67	7.17	5.76	8.70	8.15	6.48
Eu	2.47	1.93	1.80	1.99	2.04	1.71
Gd	7.25	6.53	5.68	7.12	7.01	5.58
Tb	0.88	0.79	0.68	0.88	0.88	0.72
Dy	4.73	4.37	3.75	4.92	4.84	3.95
Ho	0.77	0.72	0.59	0.80	0.77	0.68
Er	2.21	2.06	1.65	2.27	2.23	1.93
Tm	0.27	0.25	0.20	0.28	0.27	0.26
Yb	1.76	1.64	1.23	1.70	1.70	1.60
Lu	0.24	0.22	0.17	0.22	0.23	0.23
ΣREE	350.6	327.6	318.8	370.9	322.7	243.3
Eu/Eu*	1.01	0.86	0.96	0.77	0.83	0.87
$(La/Yb)_N$	35.0	35.0	49.5	38.0	32.0	24.9

similar chondrite-normalized (based on the recommended values of Boynton (1984)) REE pattern (Fig. 5). They all show light rare earth element (LREE)-enriched pattern ($(La/Yb)_N$=25~166) with weak Eu anomaly (Eu/Eu*=0.83~1.42). The total REE concentration of the DBGD is the highest in the Daebo granites.

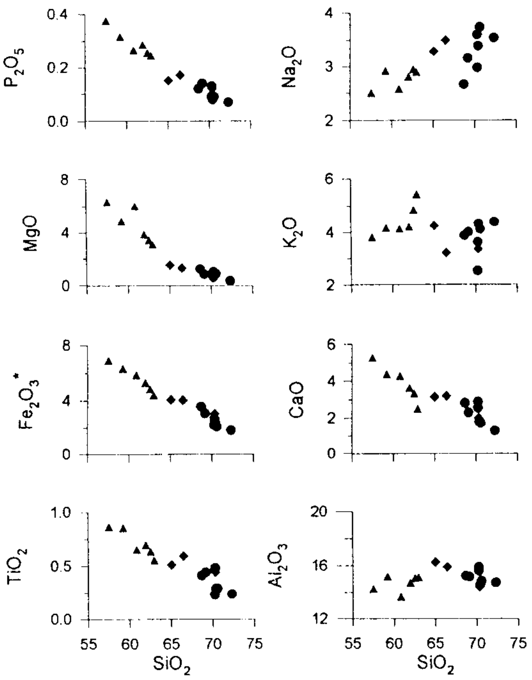

Fig. 3. Major element variation diagrams for the Daebo granites. Symbols: closed circle (DBBG), closed diamond (DBKG), and closed triangle (DBGD).

PETROGENETIC IMPLICATIONS

Tectonic Setting

Recently many geochemical schemes for tectonic discrimination of granites have been proposed (Brown *et al.*, 1984; Pearce *et al.*, 1984; Harris *et al.*, 1986; Maniar and Piccoli, 1989; Barbarin, 1990), but difficulties arise from the complicated petrogenetic history of granites. The involvement of geochemically distinct geologic reservoirs in different tectonic environments could be reflected in some geochemical indicators of granites, however.

When plotted on tectonic discrimination diagram of Pearce *et al.* (1984) (Fig. 6), most Daebo granite samples fall in the volcanic arc granite field. Data of the PTGR (Cheong and Chang, 1996) are also plotted in Figure 6 for comparison. Volcanic arc granite and post-collisional granite show quite similar geochemical characteristics, but Ta concentration of

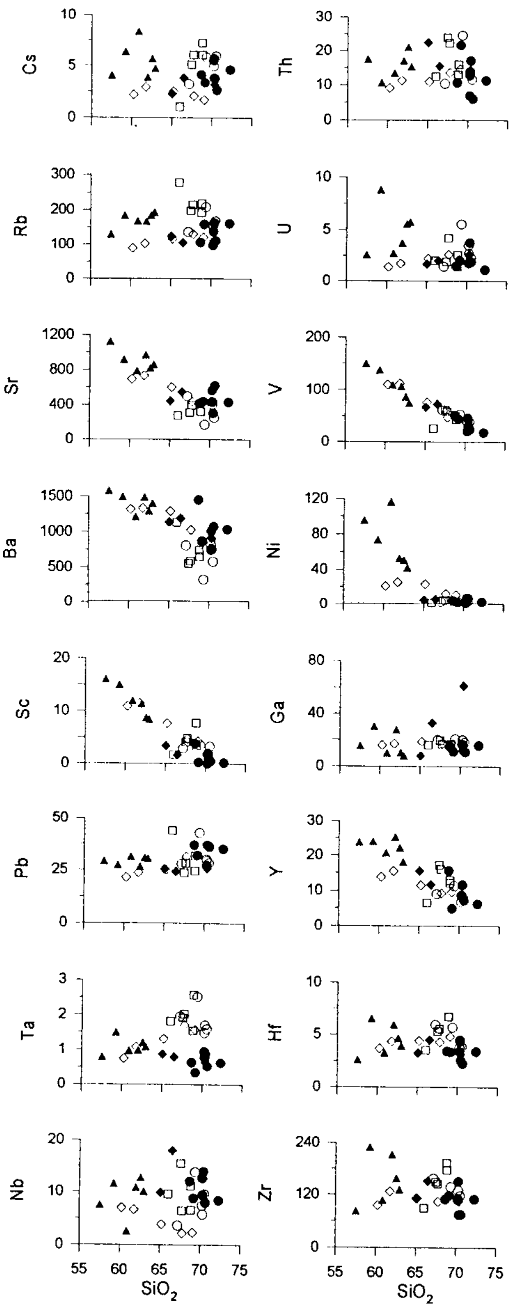

Fig. 4. Trace element variation diagrams for the granites. Symbols of the Daebo granites are the same as in Fig. 3. Symbols of Permian to Triassic granites near the Boeun area (Cheong and Chang, 1996): open diamond; Baegrock Granodiorite, open circle; Boeun Granite, open square; Chungsan Granite.

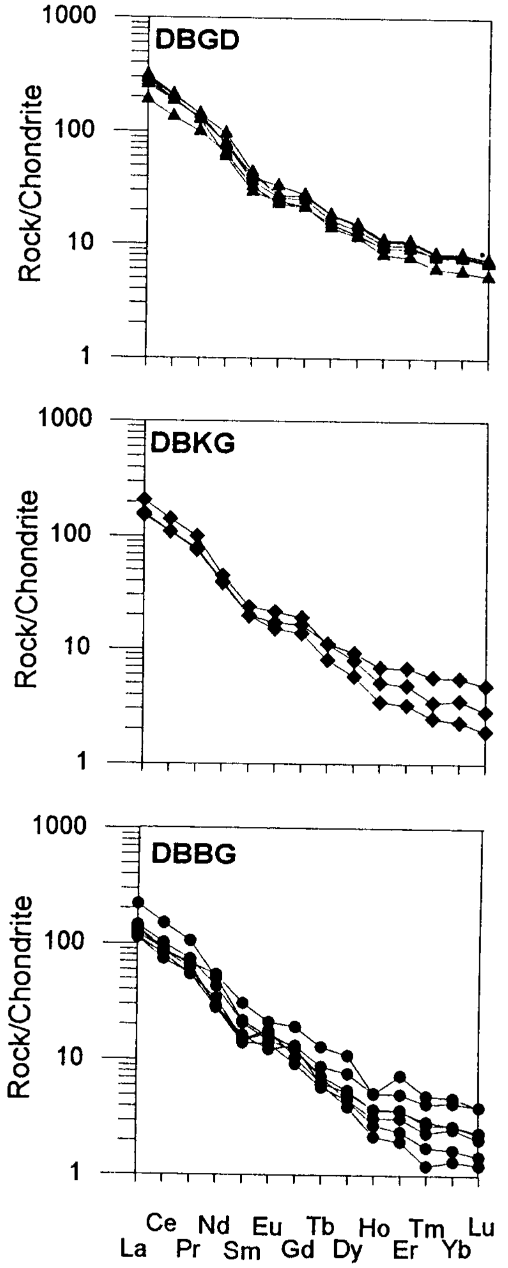

Fig. 5. Chondrite normalized REE patterns of the Daebo granites.

the former tends to be lower, although not all post-collisional granites demonstrate distinct Ta enrichment (Harris *et al.*, 1986). The Daebo granites and the PTGR occupy different fields in the Hf-Rb/30-Ta x 3 diagram (Harris *et al.*, 1986) (Fig. 7). The Boeun Granite and the Chungsan Granite of the PTGR lie in the late and post-collisional granite field resulted from their high Ta/Hf ratios. The Daebo granites and some Baegrock Granodiorite samples lie

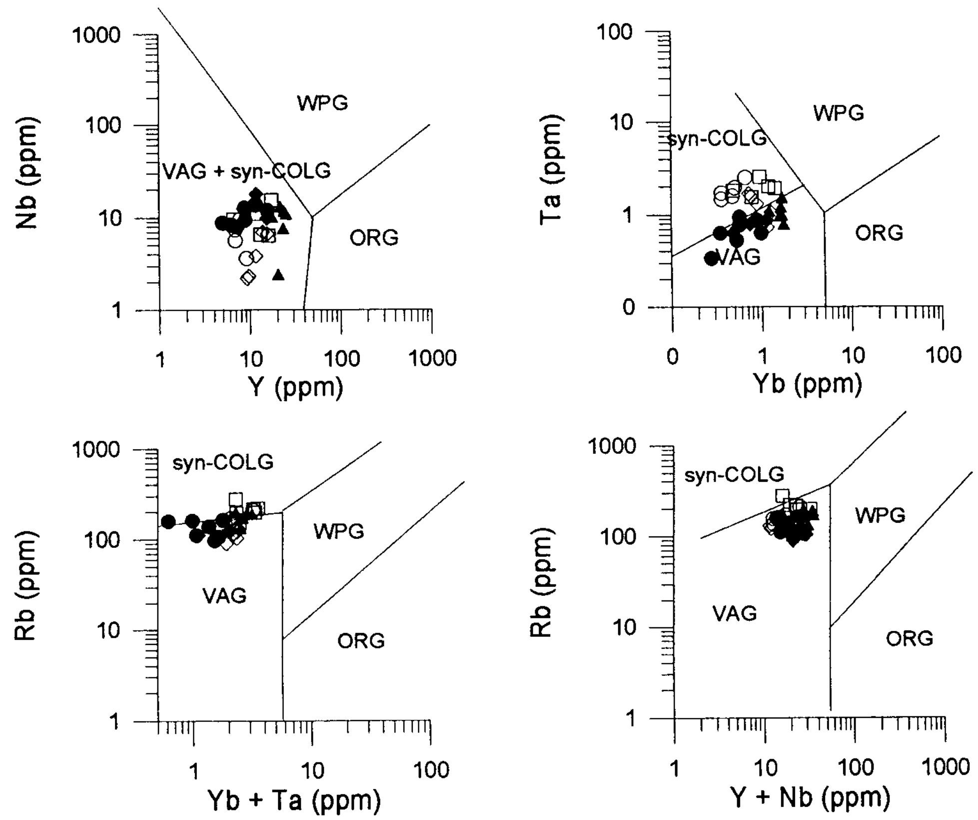

Fig. 6. Tectonic discrimination diagrams (Pearce et al., 1984). Abbreviations: VAG (volcanic arc granite), syn-COLG (syn-collisional granite), ORG (oceanic ridge granite), and WPG (within plate granite). Symbols are the same as in Fig. 4.

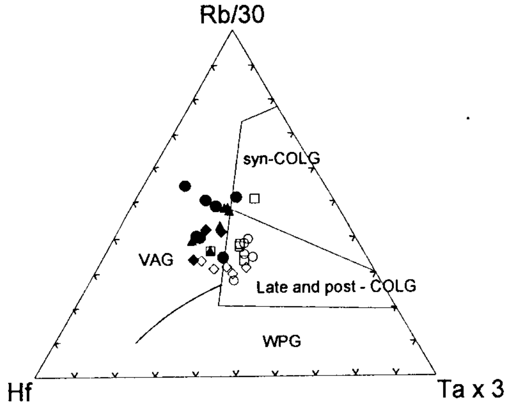

Fig. 7. Tectonic discrimination diagram (Harris *et al.*, 1986). Symbols are the same as in Fig. 4.

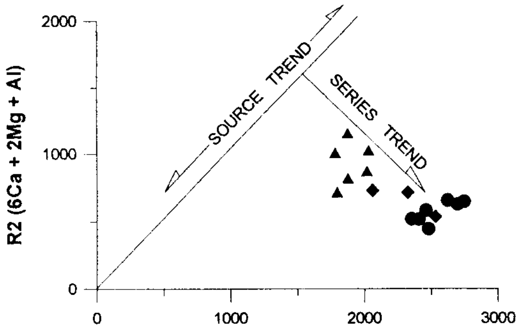

Fig. 8. The de la Roche R1-R2 multicationic diagram. Symbols are the same as in Fig. 3.

in the volcanic arc granite field because of their relatively lower Ta/Hf ratios. LIL element concentrations of the Daebo granites are much higher than those of the Baegrock Granodiorite. But HFS elements (Ta, Hf, Nb, and Y) are not distinguishably enriched in the former. This indicates that the Daebo granites were formed in a normal calc-alkaline continental arc system, and the Baegrock Granodiorite in a more primitive arc system (Brown *et. al.*, 1984).

Source Heterogeneity

The variations of Na and K in the granites can not be explained by simple fractional crystallization from the same primary magma. The irregular behavior of these alkali elements indicates a variety of source materials or incomplete mixing of different source materials. The variation of Na and K could be related to the involvement of different source materials during and after orogenic cycles (Batchelor and Bowden, 1985). When plotted on a de la Roche (1980) R1-R2 multicationic diagram (Fig. 8), the granites display rather scattered pattern. In Figure 8, the source trend (related to the mixing of a common source) and the series trend (related to the magmatic differentiation) suggested by Batchelor and Bowden (1985) are also shown. The DBGD does not exhibit systematic variation. Neither internal differentiation nor mixing process alone can result in this pattern. A combination of differentiation and mixing was involved, or the source material in the formation of the DBGD itself was heterogeneous. The DBKG shows series trend-like variation in the plot, although only three points were analyzed. The DBBG shows the source trend well in the plot, but it is not clear whether this signature is the result of mixing or heterogeneous source material.

The total REE concentration of the DBGD is the highest in the investigated granitoids. The DBBG does not show more evolved REE pattern (i.e. higher $(La/Yb)_N$ values or stronger Eu (-) anomaly) compared with the DBGD. Therefore it seems to be unreasonable to regard the DBBG as a late stage differentiate formed by residual melts after the fractionation of major constituent minerals of the DBGD such as hornblende and feldspar.

The LIL element variations of the Daebo granites do not match with their $\varepsilon_{Nd}(t)$ values (Fig. 9) $\varepsilon_{Nd}(t)$ values from Cheong and Chang, *in preparation*; the age of the Daebo granites was assumed to be 180 Ma in the calculation of $\varepsilon_{Nd}(t)$ values). For comparison, data of the PTGR (Cheong and Chang, 1996) are also plotted in Figure 9. As shown in Figure 9, Rb and Th concentrations of the PTGR are roughly correlated with their $\varepsilon_{Nd}(t)$ values, which implies a mixing relation between primitive magma and LIL element-enriched upper crustal materials. Cs and U concentrations of the granites are too low to show such variation. The Daebo granites do not show any consistent trend in Figure 9. This lack of consistency in isotopic and geochemical characeteristic does not support a mixing relation.

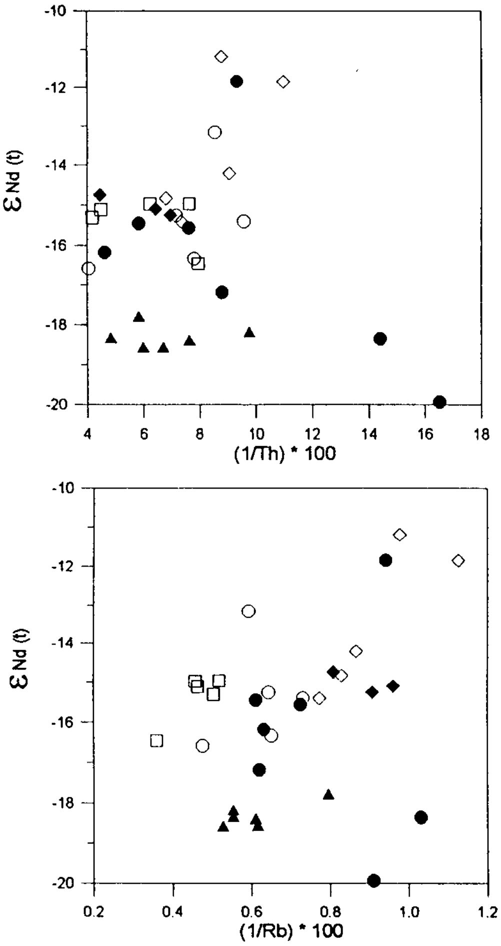

Fig. 9. $\varepsilon_{Nd}(t)$ values (Cheong and Chang, *in preparation*) against two incompatible element (Th and Rb) concentrations for the Daebo granites and the PTGR (Cheong and Chang, 1996). Roughly linear trends of the PTGR indicate a mixing relation between primitive magma and LIL element-enriched crustal materials. The Daebo granites do not show any consistent trend in these diagrams. Symbols are the same as in Fig. 4.

In summary, inconsistent variations in isotopic ratios and elemental concentrations of the Daebo granites can not be explained by simple fractional crystallization from the same primary magma. The irregular isotopic and elemental variation of the Daebo granites is taken to be inherited from an already heterogeneous source region.

CONCLUSION

LIL element-enrichment and low Ta/Hf ratios of the Daebo granitic batholith in the central Ogcheon Belt correspond to typical characteristics of normal, calc-alkaline continental arc granitoids. The irregular behavior of major alkali elements and REE patterns in the Daebo granites can not be explained by simple fractional crystallization. Inconsistent variations in $\varepsilon_{Nd}(t)$ and LIL element concentrations of the Daebo granites preclude a mixing model between primitive melt and LIL element-enriched upper crustal materials. The irregular isotopic and elemental variation of the granites is taken to be inherited from an already heterogeneous source region.

ACKNOWLEDGEMENTS

This research was supported by a grant from the Center for Mineral Resources Research. The authors thank to Professor Yongju Jwa of Gyongsang University for his careful review of this manuscript. Mr. Mansik Choi and Dr. Chansu Park of the Korea Basic Science Institute helped the first author in major and trace element analysis. Dr. Kye-Hun Park and Dr. Insung Lee of the KBSI are thanked for their valuable comments on the manuscript. Mr. Junghun Choi of Seoul National University generously allowed us to use his unpublished geologic map.

REFERENCES

Barbarin, B. (1990) Granitoid; Main petrogenetic classifications in relation to origin and tectonic settings. Geol. J., v. 25, p. 227-238.

Batchelor, R.A. and Bowden, P. (1985) Petrogenetic interpretation of granitoid rock series using multicationic parameters. Chem. Geol., v. 48, p. 43-55.

Boynton, W.V. (1984) Geochemistry of the rare earth elements: meteorite studies. In: Rare earth element geochemistry (Edited by Henderson, P.). Elsevier, p. 63-107.

Brown, G.C., Thorpe, R.S. and Webb, P.C. (1984) The geochemical characteristics of granitoids in contrasting arcs and comments on magma sources. J. Geol. Soc. London, v. 141, p. 413-426.

Cheong, C.S. and Chang, H.W. (1996) Tectono -magmatism, -metamorphism, and -mineralization of the central Ogcheon Belt (I): Sr, Nd, and Pb isotopic systematics and geochemistry of granitic rocks in the Boeun area. J. Geol. Soc. Korea, v. 32, p. 91-116.

Choo, S.H., Lee, D.J. and Kim, D.H. (1979) Rb/Sr age determination on the granitic rocks distributed around Cheongju area, central part of Korean peninsula. KIGAM report 6, Korea Institute of Geology, Mining & Materials, p. 111-132.

Choo, S.H. and Kim, S.J. (1985) A study of Rb-Sr age determinations on the Ryeong Nam Massif (I): Pyeonghae, Buncheon and Kimcheon granite gneisses. KIER report 85-24, Korea Institute of Energy and Resources, p. 7-39.

Clarke, D.B. (1992) Granitoid rocks. Chapman & Hall, 283p.

de la Roche H., Leterrier, J., Grand Claude, P. and Marchal, M. (1980) A classification of volcanic and plutonic rocks using R1-R2 diagrams and major element analysis-its relationships with current nomenclature. Chem. Geol., v. 29, p. 183-210.

DePaolo, D.J. (1981) Trace element and isotopic effects of combined wall rock assimilation and fractional crystallization. Earth Palnet. Sci. Lett., v. 53, p. 189-202.

Harris, N.B.W., Pearce, J.A. and Tindle, A.G. (1986) Geochemical characteristics of collision-zone magmatism. *In*: Collision tectonics (Edited by Coward, M.P. and Reis, A.C.). Spec. Publ. Geol. Soc., v. 19, p. 67-81.

Hibbard, M.J. (1979) Myrmekite as a marker between preaqueous and postaqueous phase saturation in granitic systems. Geol. Soc. Am. Bull., v. 90, p. 1047-1062.

Hibbard, M.J. (1995) Petrography to petrogenesis. Prentice Hall, 587p.

Hong, Y.K. (1987) Geochemical characteristics of Precambrian, Jurassic and Cretaceous granites in Korea. J. Korean Inst. Mining Geol., v. 20, p. 35-60.

Jin, M.S. (1995) Petrological and geochemical characteristics of the Mesozoic granites and their igneous activities in the Ogcheon fold belt. *In*: Geology of southwestern Ogcheon zone. Memoirs for Prof. Jong Hyuk Lees retire, p. 179-207.

Kim, O.J. (1971) Study on the intrusion epochs of younger granites and their bearing to orogenies in South Korea. J. Korean Inst. Mining Geol., v. 4, p. 1-9.

Kwon, C.S. (1988) Abundances of trace elements of the granitic rocks and their tectonic implications in Daejeon-Gongju area. J. Geol. Soc. Korea, v. 24, p. 147-162.

Kwon, S.T. (1991) Sm-Nd isotopic study of the Phanerozoic granites in South Korea: Investigation on the genesis and structure of the crust. J. Geol. Soc. Korea, v. 27, p. 528-529 (*Abstract*).

Kwon, S.T. (1992) Pb isotopic study of the Phanerozoic granites in South Korea: A preliminary report. J. Geol. Soc. Korea, v. 28, p. 514 (*Abstract*).

Maniar, P.D. and Piccoli, P.M. (1989) Tectonic discrimination of granitoids. Geol. Soc. Am. Bull., v. 101, p. 635-643.

Na, C.K. (1994) Genesis of granitoid batholiths of Okchon zone, Korea and its implications for crustal evolution. unpublished Ph.D. thesis, Univ. Tsukuba.

Pearce, J.A., Harris, N.B.W. and Tindle, A.G. (1984) Trace element discrimination diagram for the tectonic interpretation of granitic rocks. J. Petrol., v. 25, p. 956-983.

Simpson, C. and Wintsch, R.P. (1989) Evidence for deformation-induced K-feldspar replacement by myrmekite. J. Metamorphic Geol., v. 7, p. 261-275.

Taylor, H.P. (1980) The effects of assimilation of country rocks by magmas on $^{18}O/^{16}O$ and $^{87}Sr/^{86}Sr$ systematics in igneous rocks. Earth Planet. Sci. Lett., v. 47, p. 243-254.

Totland, M., Jarvis, I. and Jarvis, K.E. (1992) An assessment of dissolution techniques for the analysis of geologic samples by plasma spectrometry. Chem. Geol., v. 95, p. 35-62.

Manuscript received 15 May 1996

중부 옥천대에 분포하는 대보 화강암질 저반의 화학조성 : 예비보고서

정창식 · 장호완

요약 : 중부 옥천대에 분포하는 대보 화강암질 저반의 주원소, 미량원소 조성으로부터 조구조환경과 기원물질의 특징을 연구하였다. 화강암류는 흑운모 화강암, 조립질 반상화강암 및 화강섬록암으로 나눌 수 있다. 화강암류의 불규칙적인 Na, K 함량변화는 분별정출작용만으로 설명될 수 없고 기원물질의 불균질성이나 다양한 기원물질의 불완전한 혼합을 반영하는 것으로 생각된다. 대보 화강암에서 나타나는 친석 원소(LIL element)의 부화와 낮은 Ta/Hf비는 정상적인 칼크 알칼리 계열의 대륙 연변부 호 화강암의 특징과 부합된다. 희토류원소 변화양상으로 보아 SiO_2 함량이 높은 흑운모 화강암을 보다 염기성인 화강섬록암의 후기 분화체로 보기는 어렵다. 대보 화강암의 $\varepsilon_{Nd}(t)$ 값과 친석 원소의 함량은 서로 체계적인 변화를 보이지 않아 그들의 지화학적 특징이 초생적인 용융체와 지각 물질 사이의 혼합에 의해 규정되었을 가능성을 배제한다. 대보 화강암의 지구화학적 특징은 주로 기원물질의 고유한 불균질성을 반영한다고 보아진다.